International Journal of Thermophysics, Vol. 23, No. 4, July 2002 (© 2002)

Development of a Magnetic Suspension Densimeter and Measurement of the Density of Toluene[1]

R. Masui[2]

The development of a magnetic suspension densimeter that has been built for measurement of the density of compressed liquid at pressures up to 30 MPa in the temperature range 20 to 150°C is described. The densimeter was first built by the author and his coworkers at NIST. We describe here further improvements made on a second system built at NMIJ based on the same principle. The densimeter uses a small coil suspended from an electronic balance. Within the coil is placed a sample cell in which the pressurized sample and a buoy, which is a permanent magnet, are enclosed. For measurement of density, balance readings are recorded (1) with the buoy at rest and (2) with the buoy in magnetic suspension. The measurement procedure is basically a hydrostatic weighing, which is simpler than those of conventional magnetic densimetry. As an example, measurements of toluene density performed as part of an inter-laboratory comparison are presented. The data agreed with reliable literature values to within a few hundredths of a per cent.

KEY WORDS: compressed liquid; densimetry; density of liquid; electronic balance; magnetic densimeter; magnetic levitation; toluene; weighing.

1. INTRODUCTION

Magnetic-suspension densimetry provides a direct and convenient way of measuring the density of pressurized liquids. A buoy made of magnetic material is suspended in the liquid by means of a magnetic field generated

[1] Paper presented at the Fourteenth Symposium on Thermophysical Properties, June 25–30, 2000, Boulder, Colorado, U.S.A.

[2] Material Properties and Metrological Statistics Division, National Metrology Institute of Japan/AIST Tsukuba Central 3, Tsukuba, Ibaraki 305-8565, Japan. E-mail: Ryohei-masui@aist.go.jp

0195-928X/02/0700-0921/0 © 2002 Plenum Publishing Corporation

by a field coil. The density is derived from measurement of the force required to support the buoy.

Beams [1, 2], the pioneer of magnetic densimetry, and his coworkers have proposed two methods of measuring the buoyant force in magnetic densimetry. One is to measure the coil current necessary to support the buoy. The other is to suspend the sample cell from a balance, and to determine the change in weight of the cell as the buoy is brought into support.

The first method involves an accurate positioning of the buoy with respect to the coil, because the coil current is strongly dependent on the distance from the support coil. This can be elaborate work. Furthermore, changes in magnetization of the buoy as a function of temperature have to be calibrated accurately. The second method does not require the buoy positioning, but it is not a simple matter to weigh precisely a sample cell with attached fill lines.

The magnetic densimeter we present here uses a third method in which the support coil, instead of the cell, is weighed. It is free from the disadvantages of the above two methods, and provides a method to measure the density of pressurized liquids easily and quickly. The method was first developed by the present author and his coworkers in 1981, and a system was built at NIST. The basic principles, and comparisons with conventional methods, are described in Refs. 3 and 4. It has not been used for practical purposes, however, because an undesirable interaction between the buoy and a neighboring component was observed (as described later) which killed the advantages of the new method.

Here, we present a brief description of further development of the densimeter. We built a new magnetic densimeter of the same type at the National Metrology Institute of Japan (NMIJ/AIST). After several improvements, we found the system worked as it was originally intended in the temperature range 20 to 150°C and pressure range 0 to 30 MPa.

As an example of measurement, we present measurements of toluene density, which we carried out as part of an inter-laboratory comparison program between six groups in NMIJ, NEL, NIST, and PTB.

2. PRINCIPLE OF OPERATION

Figure 1 illustrates the principle of the present densimeter. A small field coil hangs from a balance and surrounds a cylindrical cell. The cell contains a pressurized sample liquid and a buoy which is a permanent magnet. The purpose of this configuration is to enable a precise weighing of the buoy encapsulated in the pressure cell using a balance placed outside of the cell. It is then possible to measure the density of pressurized liquids

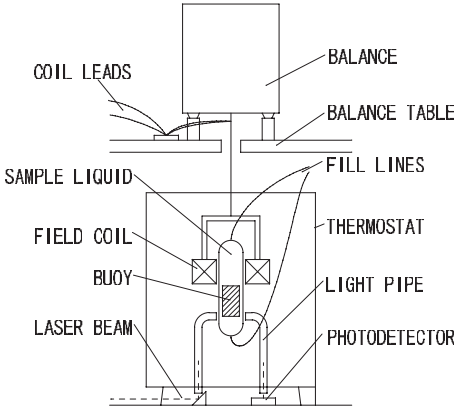

Fig. 1. Principle of magnetic syspension densimeter.

in a way similar to ordinary hydrostatic weighing. When there is no current in the coil, the buoy rests on the bottom of the cell, and the balance indicates the weight of the coil only. When the coil current is activated and the buoy is in support, the balance indicates the weight of the coil plus the apparent weight of the buoy in the sample. Therefore, the apparent weight of the buoy (F) is measured directly as a change in the balance reading as the buoy is brought into support. The density of the sample, ρ, is obtained using the relation

$$F = (m - \rho V)\, g, \tag{1}$$

where m and V are the mass and volume of the buoy, and g is the acceleration due to gravity.

Due to the nature of the magnetic field, a feedback control is necessary for stable support of the buoy. The present densimeter uses an optical sensing system which senses the vertical position of the buoy. The output signal from it controls the coil current electronically, so that the buoy is supported in a stable position.

3. APPARATUS

In this section, we will describe the major components of the densimeter. The description will be focused mainly on the improvements over the previous design [3, 4].

3.1. Balance

The balance used was an electronic balance which had a capacity of 200 g and a resolution of 0.01 mg. The beam of such a balance does not deflect on loading. This feature is essential for this application, in which we have a coil suspended from the balance whose leads have to be connected to an external current supply. Since there is no perceptible vertical motion of the coil, there is no elastic deformation in the coil leads; hence, an undesirable elastic force, which would otherwise destroy the balance sensitivity, is eliminated.

Since the sensitivity of an electronic balance can change with time, we built a computer-controlled calibration system which used a five-gram ring weight that had been calibrated against our standard weights. The balance was calibrated automatically before and after each measurement session.

3.2. Cell

The sample cell consisted of a synthetic sapphire tube of 11.7 mm O.D., 8.5 mm I.D., and 94 mm length. Sapphire was chosen for its high fracture strength at high pressures and good transparency for use with an optical sensing system. To avoid fractures due to sharp stress concentrations, the sapphire tube was mounted in such a manner that it contacted only soft Teflon components (Fig. 2).

Pressure tests confirmed that, at 200°C, the sapphire tube could take 40 MPa, which was the maximum pressure attainable with our diaphragm pump. In fact, the O-rings and the Teflon components were damaged first.

The sapphire tube was coated with yttrium oxide for better conductivity both inside and outside to discharge static electricity.

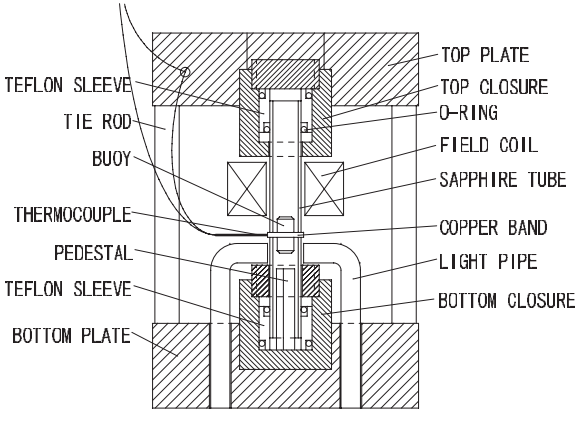

Fig. 2. Cross-sectional view of the sample cell.

3.3. Buoy and Pedestal

The buoy was a strong neodymium magnet coated with nickel (Fig. 2). It had a cylindrical shape 7 mm in diameter and 15 mm long, chamfered on both ends for protection against chipping. The nickel coating has strong resistance to corrosion in water, which enabled *in situ* measurements of the buoy volume using water as a sample.

When the buoy is not in support, it sits on a pedestal placed on the bottom of the cell. The pedestal is made of a bundle of soft gold tubes to prevent chipping of the buoy when it falls on it.

Our previous densimeter had one difficulty, that after a few months of use, a magnetic interaction developed between the buoy and the pedestal. The gold pedestal appeared to have become "magnetized," causing a height dependence of the buoy weight, which killed the major advantage of this method over Beams' first method. The same magnetization occurred if gold was replaced with tin. Removal of it required disassembly of the cell and the thermostat and replacement of the pedestal. This problem hampered practical use of this densimeter.

In the early 1990s, we built a new densimeter of the same type at NMIJ. Further investigations using it revealed that the magnetic buoy handled in an ordinary laboratory environment had many fine magnetic particles on the surface. Traces of this material were transferred to the gold pedestal after repeated dropping of the buoy onto it. We further found that the transfer of these particles could be prevented by covering the top of the pedestal with a harder metal such as copper.

Furthermore, we found that the particles turned to greyish powdery material (probably oxides) when we kept the buoy in water at 150°C and 30 MPa for several hours. The powder appeared less magnetic and could be removed easily by wiping with an alcohol-dipped swab. The present apparatus uses a buoy cleaned in this way and a copper-topped pedestal. No magnetic interaction has been observed since this improvement.

3.4. Coil and Suspension System

In order to minimize the heating of the sample due to dissipation from the coil, the coil dimension was optimized so that the maximum magnetic force was obtained with minimum heat dissipation [3]. The winding of the present coil had 16 mm I.D., 28 mm O.D., and 13 mm height. Its power consumption was 0.3 W when it supported the buoy in vacuum. The wire had polyimide coating for insulation for use at temperatures above 200°C. The coil leads were flexible silver wires. They were drawn out from the suspension system at a point near the balance bottom, and connected to an external current supply.

3.5. Feedback Control

In order to bring the buoy to a stable support, the densimeter used feedback control of the coil current. It used an optical system for position sensing.

A He-Ne laser beam was introduced into the cell through a fiber-optic light pipe. The light pipe penetrates the bottom wall of the thermostat and the bottom plate of the cell assembly. After the beam passes through a clearance under the supported buoy, another light pipe takes it out from the cell and guides it to a photodiode placed outside the thermostat. The height of the buoy is represented by the intensity of the output light, which is converted to a voltage by the diode. The voltage signal is processed by a control circuit and used to control the coil current.

For convenience of handling, the light pipe was divided into three sections, each penetrating the insulation wall, the thermostat bottom, and the bottom plate of the cell. They were aligned to each other at the same time the cell and the thermostat were assembled.

3.6. Alignment of the Axis

The buoy and the coil were aligned with the sapphire tube so that there was no mechanical contact between them. A slight deformation of the cell frame took place, however, when pressure was applied to the sample. In order to give an allowance for the displacement of the cell wall, it was desirable to support the buoy as close to the center of the cell as possible. To achieve this, the balance was placed on a precise xy-table that had no backlash. The absolute xy-coordinates of the balance were indicated on dial gauges with a resolution of 10 μm.

We achieved the axial alignment in the following way. The balance was moved in small steps in the, e.g., $+x$ direction. When the buoy reached the cell wall, a large change was observed in the balance reading. We recorded the x-coordinate of the position indicated on the dial gauge. We did the same thing in the $-x$ direction, and then the balance was brought to the middle of the two recorded positions. The entire procedure was repeated in the y-direction. In this way, the buoy was brought to the center of the sapphire tube. This procedure could be carried out even when viewing of the cell inside was not possible (e.g., when the thermostat was hot).

The axial alignment could be upset due to thermal deformation of the balance table, which is supported on four thick aluminum legs. If these legs are at different temperatures due to uneven heat leakage from the thermostat, there can be a lateral displacement of the balance with respect to

the cell. A difference of 4 K in the leg temperatures caused a displacement of about 0.1 mm. In the present apparatus, we carefully shielded the heat from the thermostat using a screen, and no non-uniform expansion of the legs, hence, no lateral displacement of the balance, was observed at 150°C, the maximum measurement temperature.

3.7. Temperature Control and Measurement

The thermostat was a thick aluminum cylindrical vessel 121 mm I.D., 160 mm O.D., and 290 mm high. Thin parallel grooves were cut in the axial direction into the outer surface of the cylinder, and heater wires enclosed in thin stainless steel tubes were embedded in them. An inductance bridge using a thermistor was used for the temperature control.

Two walls filled with 60 mm thick ceramic fiber layer were used for heat insulation. The walls were two half cylinders cut in the axial direction so that the insulation was achieved by placing them on both sides of the aluminum cylinder. Two circular disks of a similar structure were placed on the top and the bottom of the thermostat. The top disk was split to permit access for the suspension wire.

The present densimeter uses an air thermostat as opposed to the silicone oil bath in the previous design [3, 4]. We found that temperature equilibrium was attained quickly enough even if we did not have the oil in the thermostat. This is because the sample volume takes only a very small portion (less than 10 cm^3) of the total thermostat volume (3,300 cm^3).

A temperature gradient was observed to develop in the sample. With this densimeter, however, it was easy to remove it, because the sample could be stirred using support/drop motions of the buoy.

Another problem with the air thermostat is temperature measurement. Because of the poor thermal contact, it is essential to place the sensor in direct contact with the sample. A platinum resistance thermometer (PRT) calibrated at NMIJ was mounted in a hole drilled in a thick aluminum block which was a part of the cell frame. A copper-constantan thermocouple was used to measure the temperature difference between the PRT and the cell. The cell had a thick copper band tightly wound around it, and one side of the thermocouple was soldered to it. The other side of the thermocouple was inserted in a hole drilled close to the PRT. Since constantan contains nickel, which is magnetic, the copper band was placed at a position at the middle of the levitated buoy so that the magnetic interaction between the buoy and the constantan became negligible. The thermocouple leads were drawn out in a direction perpendicular to the cell axis.

The stability of temperature control was 3 mK over 10 h at 50°C, 10 mK over 10 h at 100°C, and 20 mK over 10 h at 150°C. The maximum

temperature difference detected by the thermocouple was 1.6 K at 150°C. When the sample temperature was changed, a new temperature equilibrium was reached typically in four hours.

3.8. Pressure Measurement

We measured the pressure using a quartz pressure gauge which had a range of 40 MPa and an uncertainty of 5 kPa. The gauge was calibrated against Japan's national standard by the Pressure Standard Laboratory of NMIJ.

4. MEASUREMENT OF THE DENSITY OF TOLUENE

4.1. Method

We determined the volume of the buoy (V) as a function of temperature and pressure by weighing the buoy in water at 27 points in the range 24 to 150°C and 0.1 to 30 MPa. We used the IAPWS Formulation of 1995 [7] to calculate the density of water. A linear function of both temperature and pressure was least-squares fitted to the volume data.

The toluene sample was purified and supplied by NIST (Boulder) for the inter-laboratory comparison. Measurements were performed on sixteen isotherms in a sequence, 25, 40, 25, 70, 50, 130, 110, 90, 150, 140, 120, 100, 80, 60, 150, and 30°C, at four pressures, 0.1, 10, 20, and 30 MPa. Two isotherms, 25, and 150°C, were measured twice for replication. A measurement session at one point consisted of 15 series, each consisting of 12 cycles of buoy support/drop operations. A session took approximately one hour. Measurement of one isotherm took a day. The balance was calibrated before and after each measurement session.

We carried out two in-vacuum weighings of the buoy, one before the in-water measurements, and one before the in-toluene measurements. The results of these two weighings were in agreement to within 0.02 mg, indicating that the mass of the buoy was sufficiently stable. Using the mean of these values as the true mass of the buoy (m), the density was calculated using Eq. (1).

4.2. Results

Table I lists the measurement results. We fitted the following function to the density data using the least-squares method. This function was

Table I. Results, Including a Comparison to Values Calculated with Eq. (2)

Temperature (°C)	Pressure (MPa)	Density ($kg \cdot m^{-3}$)		
		Measured	Calculated	Residuals
25.523	0.104	862.10	861.95	0.15
25.773	9.832	869.10	869.20	−0.10
26.026	19.812	875.90	876.06	−0.16
26.307	29.991	882.28	882.47	−0.19
41.522	0.039	846.93	846.85	0.08
41.575	10.052	855.17	855.28	−0.11
41.601	20.027	863.14	862.94	0.20
41.633	29.599	869.67	869.65	0.02
25.032	0.047	862.28	862.36	−0.08
25.216	10.218	869.82	869.98	−0.16
25.461	20.073	876.62	876.72	−0.10
25.741	29.866	883.12	882.86	0.26
69.394	0.283	820.66	820.64	0.02
69.478	10.270	830.70	830.58	0.12
69.488	19.883	839.28	839.20	0.08
69.512	29.910	847.38	847.26	0.12
51.349	0.981	838.41	838.49	−0.08
51.418	9.987	846.33	846.46	−0.13
51.438	20.018	854.49	854.60	−0.11
51.430	29.944	861.95	861.92	0.03
130.547	0.821	759.18	759.13	0.05
130.549	10.189	773.49	773.37	0.12
130.576	20.040	786.13	786.10	0.03
130.587	30.105	797.55	797.32	0.23
110.754	1.081	780.61	780.52	0.09
110.778	10.214	792.63	792.47	0.16
110.813	19.953	803.47	803.57	−0.10
110.853	29.967	813.40	813.54	−0.14
88.152	0.558	802.39	802.67	−0.28
88.252	10.373	813.74	813.66	0.08
88.296	20.121	823.08	823.34	−0.26
88.320	30.174	832.26	832.21	0.05
149.882	1.121	738.34	738.36	−0.02
149.884	10.390	754.44	754.62	−0.18
149.886	19.954	768.68	768.70	−0.02
149.869	30.101	781.29	781.46	−0.17
140.507	0.960	748.46	748.47	−0.01
140.536	10.472	764.26	763.97	0.29
140.523	20.215	777.19	777.40	−0.21
140.507	29.971	788.93	788.98	−0.05

Table I. *(Continued)*

Temperature (°C)	Pressure (MPa)	Density ($kg \cdot m^{-3}$)		
		Measured	Calculated	Residuals
120.762	1.556	770.57	770.80	−0.23
120.768	10.334	782.87	783.06	−0.19
120.751	19.825	794.46	794.62	−0.16
120.790	30.016	805.40	805.36	0.04
111.584	0.845	778.99	779.31	−0.32
99.029	0.885	792.45	792.23	0.22
99.044	10.155	803.42	803.45	−0.03
99.050	19.159	813.68	813.08	0.60
99.084	29.899	823.19	823.18	0.01
78.598	0.149	811.71	811.55	0.16
78.649	10.234	822.19	822.27	−0.08
78.692	19.939	831.33	831.41	−0.08
78.715	29.943	839.88	839.82	0.06
60.548	0.136	829.05	828.94	0.11
60.614	10.317	838.29	838.55	−0.26
60.636	19.853	846.61	846.68	−0.07
60.628	29.620	854.11	854.23	−0.12
149.895	1.533	739.19	739.19	0.00
149.890	10.088	754.38	754.13	0.25
149.893	20.164	769.03	768.97	0.06
149.877	29.901	781.25	781.23	0.02
30.211	0.050	857.78	857.50	0.28
30.295	10.374	865.69	865.57	0.12
30.326	19.907	872.47	872.45	0.02
30.329	29.810	879.10	879.04	0.06

developed by Watson [5] who used it to represent the density data of toluene measured by Magee and Bruno [6].

$$\Psi = A_1 + \theta^2[\theta^{0.5}(A_2 + A_4\theta + A_5\theta^{10}) + A_3\theta] + A_6\pi^{0.5}\theta^{10} + \pi\theta[A_7 + A_8\theta^3 + \pi\theta^{2.5}(A_9 + A_{10}\pi^3\theta^{1.5})] \quad (2)$$

where Ψ is a reduced density, $\Psi = \rho/\rho_0$;

θ is a reduced temperature, $\theta = T/T_0$;

π is a reduced pressure, $\pi = p/p_0$; and

$\rho_0 = 1000\ kg \cdot m^{-3}$, $T_0 = 300\ K$, $p_0 = 10\ MPa$.

The coefficients obtained are given in Table II.

Table II. Coefficients of Eq. (2)

A_1	1.098821532144
A_2	-1.895730315482
A_3	2.690529609454
A_4	-1.033131300110
A_5	$1.201484561946 \times 10^{-4}$
A_6	$1.006045440184 \times 10^{-4}$
A_7	$5.920361358889 \times 10^{-3}$
A_8	$2.017542214553 \times 10^{-3}$
A_9	$-2.862356439342 \times 10^{-4}$
A_{10}	$1.712794786980 \times 10^{-8}$

Comparisons with other participants of the inter-laboratory comparison are not available, because the program has not yet been completed at the time of writing. Table III compares the values calculated using this equation with the Magee and Bruno data [6]. Magee and Bruno values were calculated using a Watson-type function which we least-squares fitted to their data in the temperature range 25 to 125°C.

4.3. Uncertainties

The residuals of the fitting were regarded as random fluctuations, the rms of which was 0.16 $kg \cdot m^{-3}$. The systematic part of the uncertainty was as follows. The five-gram ring weight used for balance calibration was calibrated against our standard weights to an uncertainty of 35 μg. The function representing the buoy volume had an uncertainty due to uncertainties in the parameters determined by least-squares fitting. The maximum of such uncertainty was estimated to be 0.00008 cm^3. The uncertainty involved in the IAPWS formulation for water was negligible. The toluene sample was carefully purified at NIST. We transferred it into the densimeter in vacuum. The densimeter was first cleaned with toluene at 150°C. We therefore assumed that the contribution from impurities was negligibly small. The pressure gauge is traceable to NMIJ standards to an uncertainty of 5 kPa.

Uncertainties in temperature measurement need careful considerations, because it is difficult to estimate the temperature difference between the enclosed sample and the outside sensor by direct measurements. The temperature gradient within the cell was assumed to be negligible, because the sample was stirred by the frequent support/drop operation of the buoy which was a part of the measurement procedure itself. During a measurement session, the temperature of the cell rose slowly (average rate $\simeq 0.003$ $K \cdot min^{-1}$) due to dissipation from the coil, and the drift amounted

Table III. Comparison with Data of Magee and Bruno [6]

Temperature (°C)	Pressure (MPa)	MB equation ($kg \cdot m^{-3}$)	Present Meas. ($kg \cdot m^{-3}$)	Diff. ($kg \cdot m^{-3}$)
25	0.100	861.88	862.44	−0.56
25	10.000	869.43	870.02	−0.59
25	20.000	876.48	877.07	−0.59
25	30.000	883.04	883.55	−0.52
30	0.100	857.20	857.74	−0.54
30	10.000	864.97	865.55	−0.58
30	20.000	872.22	872.79	−0.57
30	30.000	878.93	879.43	−0.50
40	0.100	847.80	848.34	−0.55
40	10.000	856.05	856.64	−0.59
40	20.000	863.69	864.28	−0.59
40	30.000	870.73	871.24	−0.51
50	0.100	838.32	838.92	−0.59
50	10.000	847.10	847.74	−0.64
50	20.000	855.16	855.81	−0.65
50	30.000	862.55	863.11	−0.56
60	0.100	828.76	829.43	−0.66
60	10.000	838.10	838.82	−0.72
60	20.000	846.61	847.34	−0.73
60	30.000	854.38	855.02	−0.64
70	0.100	819.10	819.84	−0.74
70	10.000	829.05	829.85	−0.80
70	20.000	838.05	838.87	−0.82
70	30.000	846.21	846.93	−0.72
80	0.100	809.30	810.12	−0.82
80	10.000	819.93	820.81	−0.88
80	20.000	829.45	830.35	−0.90
80	30.000	838.04	838.83	−0.79
90	0.100	799.35	800.22	−0.87
90	10.000	810.72	811.66	−0.94
90	20.000	820.80	821.76	−0.96
90	30.000	829.86	830.69	−0.83
100	0.100	789.22	790.12	−0.90
100	10.000	801.41	802.38	−0.96
100	20.000	812.11	813.10	−0.99
100	30.000	821.67	822.51	−0.85
110	0.100	778.88	779.78	−0.89
110	10.000	792.00	792.95	−0.95
110	20.000	803.37	804.34	−0.97
110	30.000	813.47	814.28	−0.81
120	0.100	768.32	769.18	−0.86
120	10.000	782.46	783.37	−0.91
120	20.000	794.56	795.49	−0.93
120	30.000	805.26	806.00	−0.75
125	0.100	762.94	763.78	−0.84
125	10.000	777.65	778.52	−0.88
125	20.000	790.14	791.03	−0.89
125	30.000	801.15	801.85	−0.70

to 0.2 K at the end of a one-hour measurement session. We measured the temperature six times at 12-minute intervals in a session. The mean of these measurements was found to represent the true mean temperature to an uncertainty of 0.005 K. Together with the PRT calibration error (0.003 K at 100°C), the combined systematic error was estimated to be 0.006 K. This uncertainty is for the temperature at the thermocouple junction.

It is necessary to estimate how well the temperature of the thermocouple junction represents the true cell temperature. Since the response of the thermocouple was sufficiently fast (time constant $\simeq 5$ s) compared to the above-mentioned drift rate, the temperature difference between the thermocouple and the cell due to response delay was negligible. If the thermal contact between the copper band and the sapphire tube is insufficient, the thermocouple reading is affected by radiation from various parts of the thermostat whose temperatures are different from that of the cell. In order to evaluate this effect, we temporarily mounted a second copper ring adjacent to the first one. We improved the degree of thermal contact of the first ring using silicone grease while keeping the contact of the second ring unchanged. We observed the temperature difference of the two rings using a thermocouple at several temperatures. It was found that the difference in the ring temperatures with and without silicone grease was about 0.050 K at 150°C, 0.015 K at 100°C, and less at lower temperatures. Since we did not use silicone grease in the measurements of toluene, we included the maximum of these values as a part of the uncertainties in the temperature

Table IV. Uncertainties of Measurement

Error factors	Uncertainties	Uncertainties in density ($kg \cdot m^{-3}$)	Uncertainties in density (%)
Random		0.16	0.019
Systematic			
Balance calibration	35 μg		
Temperature	0.056 K	0.057	0.0071
Effect of radiation	0.05 K		
Heat from the coil	0.01 K		
PRT calibration	0.003 K		
Averaging procedure	0.005 K		
Pressure	5 kPa	0.0054	0.0007
Buoy volume	0.00008 cm^3	0.12	0.014
Impurity	$\simeq$ negligible	0	0
Combined standard uncertainty		0.20	0.025

measurement, assuming that heat resistance of the thin silicone grease layer was negligibly small.

We used a similar method to estimate the effect of radiation from the coil on the temperature of the thermocouple junction. We again used a second copper ring which was placed away from the coil. Difference in temperature rises of the two rings during a measurement session represents the difference in the effect of radiation from the coil. We found that the first ring was heated 0.006 to 0.010 K more than the second ring at the end of a one-hour measurement session. We added 0.010 K to the uncertainty list as the uncertainty due to this cause.

Table IV summarizes the uncertainties of the measurement.

5. CONCLUSIONS

We conclude that a magnetic-suspension densimeter in which the support coil is suspended from a balance can measure densities of pressurized liquids with an uncertainty of a few hundredths of a per cent. Since the densimeter does not need accurate positioning of the buoy with respect to the coil, the measurement procedure was simple and rapid; most of it was automated. Measurement of the density of toluene showed that the results agreed with reliable literature values within the claimed accuracy in all the measurement range.

ACKNOWLEDGMENT

This work was based on a collaboration at NIST with J. M. H. Levelt Sengers, W. M. Haynes, R. F. Chang, and H. Davis. T. J. Bruno prepared the toluene sample for the inter-laboratory comparison, which was organized by J. Watson and M. McLinden. The sample fill system used in this work was a modified version of what W. M. Haynes suggested to the author. T. Kobata calibrated the pressure gauge. A. Ono and K. Fujii took care of funding and other managemental matters for this project. H. Monden provided us with valuable suggestions on machining of the high pressure components.

REFERENCES

1. J. W. Beams, C. W. Hulburt, W. E. Lotz, Jr., and R. M. Montague, Jr., *Rev. Sci. Instrum.* **26**:1181 (1955).
2. J. W. Beams and A. M. Clarke, *Rev. Sci. Instrum.* **42**:1455 (1971).
3. R. Masui, W. M. Haynes, R. F. Chang, H. A. Davis, and J. M. H. Levelt Sengers, *Rev. Sci. Instrum.* **55**:1132 (1984).

4. R. Masui, H. A. Davis, and J. M. H. Levelt Sengers, *Proc. Eighth Symp. Thermophys. Props.* **1**:128 (1982).
5. J. Watson, private communication (National Engineering Laboratory, East Kilbride, United Kingdom).
6. J. W. Magee and T. J. Bruno, *J. Chem. Eng. Data* **41**:900 (1996).
7. *Release on the IAPWS Formulation 1995 for the Thermodynamic Properties of Ordinary Water Substance for General and Scientific Use* (IAPWS, 1996); reprinted in P. R. Tremaine, P. G. Hill, D. E. Irish, and P. V. Balakrishnan, eds., *Steam, Water, and Hydro Thermal Systems: Physics and Chemistry Meeting the Needs of Industry* (NRC Research Press, Ottawa, 2000), pp. A106-A123.